

# Channel plasmon-polariton modes in V grooves filled with dielectric

Kristy C. Vernon,<sup>1</sup> Dmitri K. Gramotnev,<sup>1,a)</sup> and D. F. P. Pile<sup>2</sup>

<sup>1</sup>*Applied Optics Program, School of Physical and Chemical Sciences, Queensland University of Technology, G.P.O. Box 2434, Brisbane QLD 4001, Australia*

<sup>2</sup>*NSF Nano-Scale Science and Engineering Center, University of California, 5130 Etcheverry Hall, Berkeley, California 94720-1740, USA*

(Received 7 November 2007; accepted 14 November 2007; published online 7 February 2008)

We investigated the effect of dielectric filling in a V groove on the propagation parameters of channel plasmon-polariton (CPP) modes. In particular, existence conditions and critical groove angles, mode localization, field structure, dispersion, and propagation distances of CPP modes are analyzed as functions of dielectric permittivity inside the groove. It is demonstrated that increasing dielectric permittivity in the groove results in a rapid increase of mode localization near the tip of the groove and increase of both the critical angles that determine a range of groove angles for which CPP modes can exist. Detailed analysis of the field structure has demonstrated that the maximum of the field in a CPP mode is typically reached at a small distance from the tip of the groove. The effect of rounded tip is also investigated. © 2008 American Institute of Physics.

[DOI: [10.1063/1.2832441](https://doi.org/10.1063/1.2832441)]

## I. INTRODUCTION

Metallic nanostructures have recently been demonstrated to be one of the best available options for the design of effective subwavelength waveguides and interconnectors for highly integrated nanooptics, new optical sensors, and near-field optics.<sup>1–24</sup> This is because they offer a unique opportunity for breaking the diffraction limit of light which does not allow localization/concentration of electromagnetic waves in dielectric media into a region that is much smaller than the wavelength. Guided waves in such metallic structures are surface plasmons which are collective oscillations of electron plasma in the metal, coupled to electromagnetic waves.

A number of different types of metallic nanostructures guiding optical signals have been proposed and described.<sup>1–24</sup> However, it seems that the two best options for the design of effective plasmonic waveguides are the groove waveguides on a metal surface,<sup>12–23</sup> and gap plasmon waveguides in the form of a nanogap in a thin metal film or membrane.<sup>5–8</sup> Both these types of subwavelength plasmonic waveguides demonstrate several superior features compared to other possible guiding metallic nanostructures. These include (1) strong subwavelength localization of plasmons (the smaller the angle of the groove, or the smaller the width of the gap, the stronger the localization of the guided plasmonic eigenmodes),<sup>5,6,11,12,14</sup> (2) relatively weak dissipation and reasonable propagation distances ( $\sim 10$ – $20$  wavelengths),<sup>5,11,14–23</sup> (3) lower sensitivity to structural imperfections (because the plasmon field is largely surrounded by the metallic medium, and mode leakage is impeded by the fact that light does not propagate in the metal),<sup>16</sup> (4) compatibility with planar technology and feasibility of such nano-optical devices as interferometers, splitters, filters, etc.,<sup>16,19,20,22,23</sup> (5) broadband transmission,<sup>5,8,14,15</sup> (6) possi-

bility of single-mode operation,<sup>15</sup> and (7) even the possibility of nearly 100% transmission through sharp bends.<sup>7,8,17</sup>

Both numerical and analytical methods of analysis were developed and used for the investigation of plasmonic waveguides and devices. These methods include the finite-difference time domain approach,<sup>5–7,10,11,14–17,21,25</sup> finite element analysis,<sup>12,26</sup> effective medium approach,<sup>18,27</sup> geometrical optics approximation,<sup>28</sup> etc. Gap plasmon waveguides have been investigated in metal membranes/films surrounded by vacuum or uniform dielectric medium and in metal films on dielectric substrates.<sup>5–8</sup> However, channel plasmon-polariton (CPP) modes guided by a groove on a metal surface have so far been investigated theoretically and experimentally in vacuum grooves on metal surfaces.<sup>12,14–23</sup> At the same time, V grooves with a dielectric medium may, for example, result from fabrication procedures using metal film deposition onto dielectric wedges. It is reasonable to expect that a dielectric medium filling the groove should have a substantial impact on dispersion, dissipation, localization, and field structure of CPP modes. In particular, this expectation has been confirmed by the analytically derived lower critical taper angle of a V groove, below which CPP modes cannot exist.<sup>28</sup> This lower critical angle is proportional to the dielectric permittivity inside the groove.<sup>28</sup>

Therefore, the aim of this paper is to conduct a detailed numerical analysis of the effect of a dielectric medium in the V groove on the propagation and localization parameters of CPP modes. Dispersion, dissipation, localization, existence conditions, and field structure will be investigated as functions of dielectric permittivity inside the groove. The effect of rounded tip of the V groove on field structure and localization of the CPP mode will also be analyzed. In particular, it will be shown that the maximum of the plasmon field does not typically occur at the tip of the V groove, but rather at some small distance from it, which depends on the material

<sup>a)</sup>Electronic mail: [d.gramotnev@qut.edu.au](mailto:d.gramotnev@qut.edu.au).

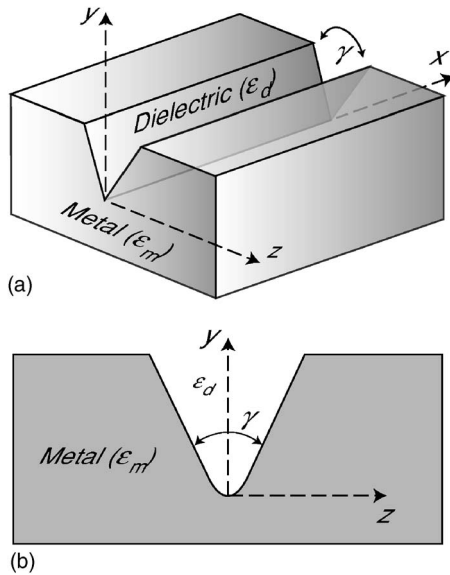


FIG. 1. (a) Metallic V groove filled with dielectric;  $\gamma$  is the taper angle of the groove,  $\epsilon_d$  is the permittivity of the dielectric inside the groove,  $\epsilon_m = e_1 + ie_2$  is the metal permittivity, and the depth of the groove in the  $y$  direction is assumed to be infinite (much larger than the penetration depth of the CPP mode up the groove). (b) The same groove, but with the rounded tip of radius  $r$ .

and structural parameters of the groove. Determination of CPP localization based on the energy consideration will be conducted.

## II. STRUCTURE AND METHODS OF ANALYSIS

The considered structure is a V groove with the angle  $\gamma$  on a metal surface (Fig. 1). The groove is filled with dielectric of the permittivity  $\epsilon_d$ , and the metal permittivity is  $\epsilon_m = e_1 + ie_2$ , where  $e_1$  and  $e_2$  are its real and imaginary parts ( $e_1 < 0, e_2 > 0$ ). The coordinate axes are as indicated in Fig. 1. The structure is considered to be infinite in the  $x$  direction, and the groove is assumed to be infinitely deep along the  $y$  axis (its depth is much larger than the penetration depth of the CPP modes along the  $y$  axis). We will primarily consider grooves with rounded tip [Fig. 1(b)] with the radius  $r$ . This is because fabrication of V-shaped grooves usually results in a rounded tip, and one of the aims of this paper is to investigate the effect of such imperfection on propagation parameters of CPP modes.

The analysis of CPP propagation in the considered structure and the effect of dielectric permittivity inside the groove is conducted using the compact-two-dimensional (2D) finite-difference time-domain (FDTD) custom-made algorithm,<sup>25</sup> geometric optics approach,<sup>28</sup> and a commercial finite-element frequency-domain (FEFD) software package (COMSOL FEMLAB). The reliability and correctness of the obtained results are verified by means of comparison of the two numerical algorithms (compact-2D FDTD and FEFD). Both the numerical approaches are used to obtain propagation distances of the CPP modes. The CPP wave numbers and field distributions inside the groove are primarily determined by means of the finite element analysis (COMSOL software package) because this approach more rapidly provides better spatial resolution and accuracy.

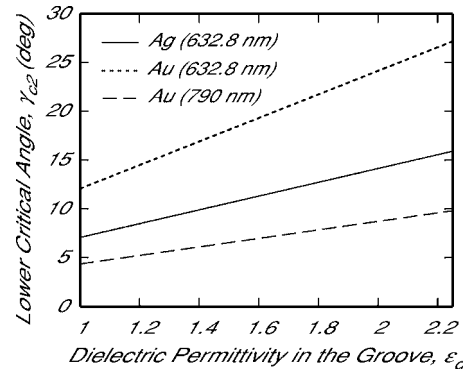


FIG. 2. The dependencies of the lower critical angle  $\gamma_{c2}$  on dielectric permittivity inside the V groove for silver (solid line) and gold (dashed and dotted lines) at the two different wavelengths. The real parts of the metal permittivities are  $e_1 = -9.50$  (gold) and  $e_1 = -16.22$  (silver) at the vacuum wavelength  $\lambda_{vac} = 632.8$  nm, and  $e_1 = -26.3$  (gold) at  $\lambda_{vac} = 790$  nm (Ref. 31).

## III. EXISTENCE CONDITIONS

As was shown previously in, Refs. 14 and 28, CPP modes in V-shaped grooves can exist only within the range of groove angles  $\gamma_{c2} < \gamma < \gamma_{c1}$ , where  $\gamma_{c1}$  and  $\gamma_{c2}$  are the upper and lower critical groove angles. A CPP mode can be represented by an antisymmetric (with respect to charge distribution across the gap) plasmon guided by the gap (V groove) with changing width.<sup>28</sup> The effective permittivity experienced by the gap plasmon decreases with increasing distance from the tip of the groove (i.e., with increasing gap width), which results in a waveguiding structure.<sup>28</sup> As a result, a CPP mode is formed by a guided gap plasmon experiencing successive reflections from the tip of the groove and the turning point (simple caustic) at some distance from the tip,<sup>28</sup> which is very similar to how a mode of a dielectric slab is formed by a bulk wave propagating in the slab and experiencing successive reflections from the slab interfaces.

If the groove angle  $\gamma$  is sufficiently small, then the conditions for adiabatic nanofocusing of plasmons in the groove are satisfied,<sup>28–30</sup> which means that the plasmon incident onto the tip of the V groove cannot be reflected back (no significant plasmon reflections occur in the adiabatic regime of nanofocusing<sup>28–30</sup>). The localization of CPP modes in this case would be infinite, and such modes do not exist.<sup>28</sup> On the other hand, if conditions for adiabatic nanofocusing are not satisfied, then the gap plasmon can be reflected from (or near) the tip of the groove and CPP modes exist.<sup>28</sup> As a result, the existence of CPP modes in a V groove [Fig. 1(a)] and adiabatic nanofocusing are antagonistic to each other.

Adiabatic nanofocusing in metallic V grooves occurs only if the groove angle  $\gamma < \gamma_{c2}$ .<sup>28–30</sup> This means that CPP modes can exist in a V groove only if<sup>28</sup>

$$\gamma > \gamma_{c2} = -2\epsilon_d/e_1. \quad (1)$$

Only if this condition is satisfied, the gap plasmon can experience reflections from the tip of the V groove and thus be guided by this groove.

Typical dependencies of lower critical groove angle  $\gamma_{c2}$  on dielectric permittivity in the groove are shown in Fig. 2 which also demonstrates typical values of  $\gamma_{c2}$  for different metals and wavelengths. In particular, it can be seen that the

lower critical angle  $\gamma_{c2}$  significantly increases with increasing dielectric permittivity in the groove and/or decreasing wavelength  $\lambda_{\text{vac}}$ . This is expected because increasing  $\epsilon_d$  results in decreasing wavelength of the gap plasmon in the groove. Therefore, at a fixed groove angle, variations of the groove width (i.e., structural parameters and plasmon wave number) within one plasmon wavelength become smaller with increasing  $\epsilon_d$ , and this means that the validity of the adiabatic approximation improves, resulting in increasing lower critical groove angle  $\gamma_{c2}$  (Fig. 2). Similarly, decreasing vacuum wavelength also results in decreasing wavelength of the gap plasmon in the groove, and this must also lead to relaxing applicability conditions for the adiabatic approximation (Fig. 2). In the same way, replacing silver by gold (at a fixed wavelength and  $\epsilon_d$ ) also leads to shorter wavelength of the gap plasmon in the groove because the magnitude of the real part of gold permittivity is smaller than that for silver. This is consistent with significantly larger lower critical angles  $\gamma_{c2}$  for gold compared to silver at the same wavelength (compare the solid and dotted lines in Fig. 2).

The obtained values of  $\gamma_{c2}$  are relatively large, and grooves with such typical angles have recently been fabricated.<sup>18–20,22,23</sup> Therefore, the lower critical angle for the determination of existence conditions of CPP modes in V grooves is important for practical applications, especially when considering grooves filled with dielectric at smaller wavelengths (larger frequencies). One should not, however, lose the sight of the fact that lower critical angle has been determined in the approximation of continuous electrodynamics and zero radius of the tip of the groove. Nonzero radius of the tip (which is inevitable in any real structure) must lead to plasmon reflections from such a tip, irrespectively of the groove angle. Nevertheless, the lower critical angle seems to provide a reasonable and useful guide for choosing geometrical parameters of groove waveguides with small radius of the tip.

As indicated in the beginning of this section and demonstrated in Refs. 12 and 14, there is also an upper critical groove angle  $\gamma_{c1}$ , above which a CPP mode does not exist. The values of this upper critical angle are significantly different for different CPP modes:  $\gamma_{c1}$  decreases with increasing order of the CPP mode. This means that the number of higher CPP modes increases with decreasing  $\gamma$ .<sup>14,15</sup> At the upper critical groove angle, the wave number of the respective CPP mode becomes equal to the wave number of surface plasmons on the sides of the groove. Therefore, if  $\gamma \geq \gamma_{c1}$ , the respective CPP mode leaks into surface plasmons on the side of the groove, and thus it stops being a structural eigenmode of the groove (see also Refs. 12, 14, and 15). No analytical equation for the upper critical angle has been obtained so far, but its values can be determined by finding groove angles at which the wave numbers of the respective CPP modes are equal to those of surface plasmons at the sides of the groove (far away from the tip, where coupling between surface plasmons at the opposite sides of the groove can be neglected). This was done using both the numerical approaches: compact-2D FDTD (Ref. 25) and FEFD.

The typical dependencies of wave numbers of the fundamental CPP mode in V-shaped grooves with rounded tip of

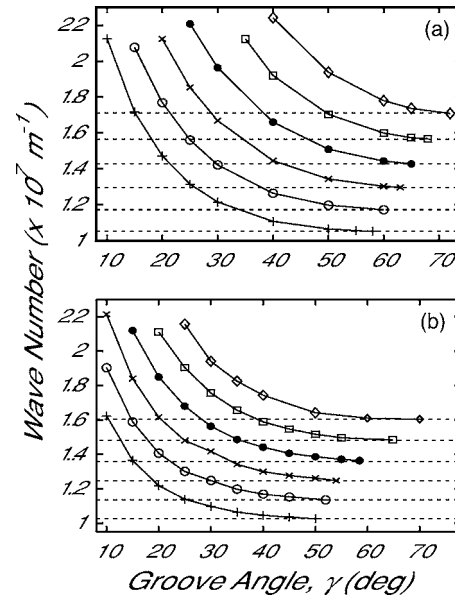


FIG. 3. Wave numbers of the fundamental CPP modes vs groove angle for a V groove with the rounded tip of radius  $r \approx 2.24$  nm in gold (a) and silver (b) at the vacuum wavelength  $\lambda_{\text{vac}} = 632.8$  nm and different values of the dielectric permittivity in the groove:  $\epsilon_d = 1$  (+),  $\epsilon_d = 1.21$  (○),  $\epsilon_d = 1.44$  (×),  $\epsilon_d = 1.69$  (●),  $\epsilon_d = 1.96$  (□), and  $\epsilon_d = 2.25$  (◇). The metal permittivities are  $\epsilon_m = -9.50 + 1.13i$  for gold and  $\epsilon_m = -16.22 + 0.52i$  for silver (Ref. 31). Dotted lines correspond to wave numbers of surface plasmons on the sides of the groove far from the tip, where coupling between surface plasmons on the opposite sides of the groove can be neglected.

radius  $r \approx 2.24$  nm in gold and silver are presented in Fig. 3 for vacuum wavelength  $\lambda_{\text{vac}} = 632.8$  nm. The rounded tip was used to enable convergence of the numerically calculated field near the tip of the groove and to make the analyzed structures more realistic. Note, however, that, as we will see below, such small rounding of the tip does not have any significant effect on CPP wave numbers if the groove angle is not too close to  $\gamma_{c2}$ .

The first important feature that can be seen from Figs. 3(a) and 3(b) is that for both the gold and silver grooves wave number of the fundamental CPP mode rapidly increases with decreasing groove angle for all values of the dielectric permittivity in the groove. Secondly, increasing  $\epsilon_d$  results in a substantial increase of CPP wave number. Thirdly, increasing groove angle results in decreasing wave number of the fundamental CPP mode, eventually reducing it to that of the surface plasmons at the sides of the groove far away from the tip. As indicated above, this determines the upper critical groove angles above which the fundamental CPP mode leaks into surface plasmons at the sides of the groove. The values of these upper critical groove angles are shown in Figs. 3(a) and 3(b) by the points of intersection between the solid curves and dashed lines corresponding to the wave numbers of surface plasmons at an isolated metal-dielectric interface for different values of  $\epsilon_d$  [see the rightmost points on the solid curves in Figs. 3(a) and 3(b)].

The dependencies of the upper critical groove angle on dielectric permittivity in the groove are presented in Fig. 4 for the same structures as in Figs. 3(a) and 3(b).

In particular, the upper critical angle  $\gamma_{c1}$  for the fundamental CPP mode in the V groove with rounded tip increases

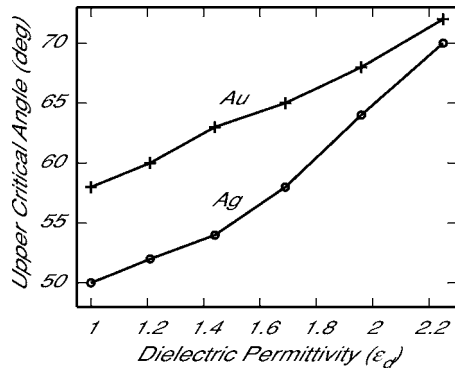


FIG. 4. The dependencies of the upper critical angle  $\gamma_{c1}$  on dielectric permittivity  $\epsilon_d$  inside the groove with the rounded tip in gold (the upper curve) and silver (the lower curve). The structural parameters are the same as for Fig. 3.

with increasing dielectric permittivity in the groove (Fig. 4). Similar situation occurs for other (higher) CPP modes in the structure with the only difference that the values of the upper critical angles for higher CPP modes decrease with increasing order of the mode. The comparison of Figs. 2 and 4 also shows that increasing dielectric permittivity in the groove results in shifting the angular range where CPP modes can exist toward larger groove angles because both the critical angles  $\gamma_{c1}$  and  $\gamma_{c2}$  increase with increasing  $\epsilon_d$ . For example, for gold with the dielectric permittivities in the groove  $\epsilon_d = 1$  (vacuum) and  $\epsilon_d = 2.25$ , the ranges of the groove angles at which CPP modes can exist are  $\sim 15^\circ < \gamma < \sim 58^\circ$  and  $\sim 30^\circ < \gamma < \sim 72^\circ$ , respectively (Figs. 2 and 4).

The numerical analysis of the dependencies of the upper critical angle on radius of curvature of the tip of the groove has demonstrated only weak dependence of  $\gamma_{c1}$  on  $r$ . For example, at  $\epsilon_d = 2.25$ , changing radius of the tip from 0.5 to 5 nm results in less than  $\sim 1\%$  variation of the CPP wave number near the critical angle. Nevertheless, it is still possible that the actual values of  $\gamma_{c1}$  shown by the curves in Fig. 4 may contain some computational errors that may be associated with computational difficulties with the numerical analysis of eigenmodes near a cutoff.

#### IV. FIELD DISTRIBUTIONS

The numerical analysis of the field distributions for the fundamental CPP mode has been conducted in grooves with different dielectric permittivities  $\epsilon_d$  and radii of the tip [Fig. 1(b)]. For example, the dependencies of magnitude of the electric field amplitude in the fundamental CPP mode in the middle of the groove on distance from the tip (i.e., on the  $y$  coordinate) are presented in Fig. 5 for the  $45^\circ$  groove in the silver substrate at three different values of the dielectric permittivity  $\epsilon_d$ .

In particular, Fig. 5 demonstrates that the field maximum in the fundamental CPP mode is achieved not exactly at the rounded tip of the groove, but rather at some small finite distance from it:  $y_{\max} \approx 5$  nm (see the insert in Fig. 5). For the considered parameters, the position of this maximum  $y_{\max}$  hardly depends on  $\epsilon_d$  (Fig. 5), but it increases with increasing radius of curvature  $r$  of the tip and decreases with increasing groove angle  $\gamma$  [Figs. 6(a) and 6(b)]. In addition,

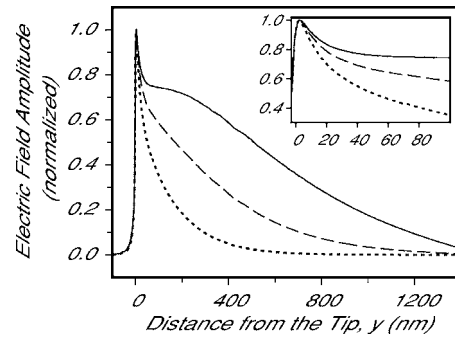


FIG. 5. The dependencies of the magnitude of the electric field amplitude in the fundamental CPP modes in the middle of the groove on distance from the rounded tip [i.e.,  $y$  coordinate, Fig. 1(b)] for the silver groove with  $\gamma = 45^\circ$ ,  $\lambda_{\text{vac}} = 632.8$  nm, radius of the tip  $r \approx 2.24$  nm,  $\epsilon_m = -16.22 + 0.52i$ , and three different values of the dielectric permittivity  $\epsilon_d = 1$  (solid curve),  $\epsilon_d = 1.44$  (dashed curve), and  $\epsilon_d = 2.25$  (dotted curve). All the three curves are normalized to the maximum of the field in the mode. The value  $y = 0$  corresponds to the rounded tip of the groove [see Fig. 1(b)].

for  $y > y_{\max}$ , field decay in the fundamental CPP mode strongly varies with increasing dielectric permittivity in the groove. Increasing  $\epsilon_d$  results in significantly stronger localization of the CPP mode near the tip. As can be seen from Fig. 5, field decay with increasing  $y$  is substantially different from purely exponential dependence, especially for smaller values of the dielectric permittivity in the groove.

The fact that the field maximum is achieved at a finite distance from the tip (rather than at the tip itself) can be explained as follows. As has been shown in Ref. 28, a CPP mode can be represented by a gap plasmon guided by the groove, i.e., by the gap with changing width (which is equivalent to changing effective permittivity experienced by the guided gap plasmon). As a result, the gap plasmon rep-

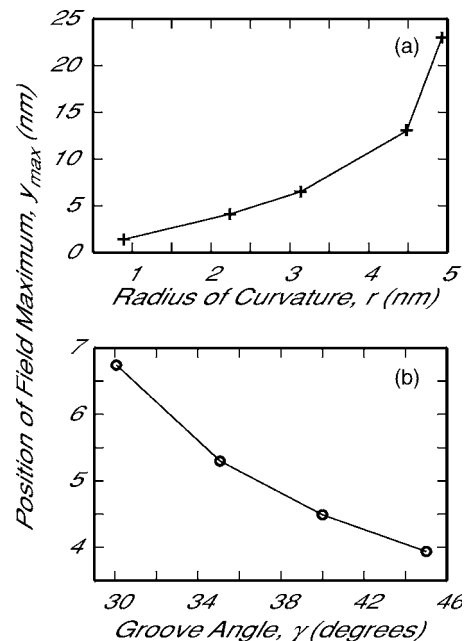


FIG. 6. The dependencies of the distance  $y_{\max}$  from the tip of the silver-vacuum grooves ( $\epsilon_d = 1$ ,  $\epsilon_m = -16.22 + 0.52i$ ) to the maximum of the electric field in the fundamental CPP mode ( $\lambda_{\text{vac}} = 632.8$  nm) on radius of curvature of the tip and groove angle. (a) Groove angle is fixed:  $\gamma = 45^\circ$ . (b) Radius of the tip is fixed:  $r \approx 2.24$  nm.



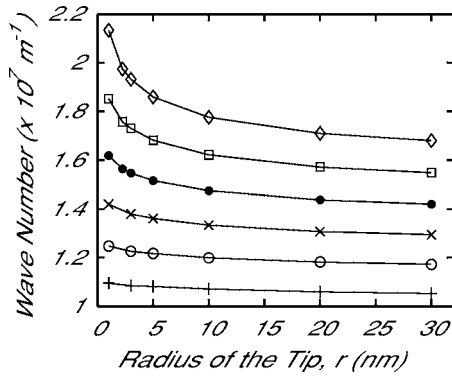


FIG. 7. The dependencies of the wave numbers of the fundamental CPP mode on radius of the tip of the  $30^\circ$  V groove in silver ( $\epsilon_m = -16.22 + 0.52i$ ) at the vacuum wavelength  $\lambda_{\text{vac}} = 632.8$  nm and different values of the dielectric permittivity in the groove:  $\epsilon_d = 1$  (+),  $\epsilon_d = 1.21$  (O),  $\epsilon_d = 1.44$  (x),  $\epsilon_d = 1.69$  (●),  $\epsilon_d = 1.96$  (□), and  $\epsilon_d = 2.25$  (◇).

representing the CPP mode experiences successive reflections from the tip of the groove and the turning point (simple caustic).<sup>28</sup> As discussed in the previous section, reflections from the tip may occur only at sufficiently large groove angles:  $\gamma > \gamma_{c2}$ , i.e., when the conditions for the adiabatic regime of plasmon propagation in the tapered gap are not satisfied.<sup>28–30</sup> In this case, the gap plasmon propagating toward the tip of the groove experiences significant reflections (due to nonadiabaticity) before it reaches the actual tip. As a result, the maximum of the field is achieved at a finite distance from the tip (Figs. 5 and 6). It is expected that decreasing groove angle to  $\sim \gamma_{c2}$  should result in  $y_{\text{max}} \rightarrow 0$  (if the tip radius  $r = 0$ ), though this is difficult to verify using the numerical approaches, because of the computational difficulties arising from the analysis of CPP modes in grooves with small taper angles that are close to the lower critical angle.

The sharp maximum at  $\sim 5$  nm from the tip on the solid curve in Fig. 5 disappears when the radius of the tip is increased above  $\sim 5$  nm. However, at the considered groove angle ( $\gamma = 45^\circ$ ), this does not have a very significant effect on CPP wave numbers, if the dielectric permittivity in the groove is small (see Fig. 7). This is because though the sharp maximum of the field at  $y = y_{\text{max}}$  is relatively high, the width of the groove (and thus the volume with the relatively large field) is small (because of the proximity to the tip). Therefore, the contribution of the sharp field maximum (solid curve in Fig. 5) to the overall energy and localization of the CPP mode is insignificant, i.e., the portion of energy corresponding to this maximum is small compared to the overall energy in the CPP mode. If the permittivity in the groove is increased, then the relative portion of the CPP energy corresponding to this field maximum also increases (compare solid and dotted curves in Fig. 5). Therefore, the effect of increasing radius of curvature of the tip plays more significant role in this case (see the higher curves in Fig. 7).

Complex pattern of the decaying field in a CPP mode with increasing distance from the tip of the groove (Fig. 5) makes inaccurate the usual determination of mode localization by the determination of the distance within which the amplitude of the field drops  $e$  times. Therefore, the direct use of the dependencies in Fig. 5 for the determination of mode

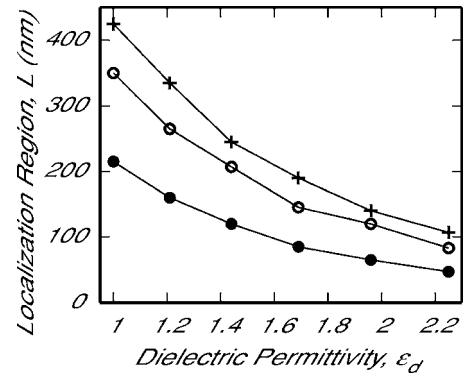


FIG. 8. The dependencies of localization region  $L$  (along the  $y$  axis) of the fundamental CPP mode in the V groove in silver with the tip radius  $r \approx 2.24$  nm at  $\lambda_{\text{vac}} = 632.8$  nm on dielectric permittivity  $\epsilon_d$  in the groove. Three different curves correspond to different groove angles:  $\gamma = 45^\circ$  (+),  $\gamma = 40^\circ$  (O), and  $\gamma = 30^\circ$  (●).

localization may be ambiguous and misleading. At the same time, physically reasonable determination of the typical localization regions is important for the design of subwavelength plasmonic waveguides. For example, this should impact the choice of the groove depth in order to achieve effective single-mode operation of the groove plasmonic waveguides.<sup>12,15,21</sup> The groove depth should be chosen so that to ensure effective guiding of the fundamental mode, while the higher modes should not be supported by the structure.<sup>12,15,21</sup> In particular, the groove depth should be chosen so that to be larger than the typical localization region for the fundamental mode along the  $y$  axis (to ensure its effective guiding<sup>12,15,21</sup>).

For accurate determination of CPP localization, we use an approach in which the region of mode localization along the  $y$  axis is determined by the distance from the tip  $L$ , such that the region  $y < L$  contains  $(1 - 1/e)$ , i.e., approximately 63% of the overall energy in the mode. The resultant dependencies of localization distance  $L$  on dielectric permittivity in the silver-vacuum groove with the tip radius  $r \approx 2.24$  nm are presented in Fig. 8 for three different groove angles and vacuum wavelength  $\lambda_{\text{vac}} = 632.8$  nm.

As expected, increasing dielectric permittivity in the groove results in decreasing  $L$ , which means increasing localization of the CPP mode. For example, for the groove angle  $\gamma = 40^\circ$  and  $\epsilon_d = 1$  (vacuum in the groove), we have  $L \approx 350$  nm, while for  $\epsilon_d = 2.25$ , mode localization is approximately four times stronger:  $L \approx 80$  nm (Fig. 8). Furthermore, decreasing groove angle also results in a significant increase of localization (Fig. 8).

Stronger localization of a CPP mode means stronger penetration of the plasmon field into the metal where dissipation occurs. This is one of the reasons why it is possible to expect decreasing propagation distance with increasing mode localization, i.e., with increasing dielectric permittivity in the groove and/or decreasing its angle. Typical propagation distances at which the electric field amplitude decreases  $e$  times are presented in Fig. 9.

Significant reduction of the propagation distance with increasing dielectric permittivity in the groove can be seen from Fig. 9. Similar situation occurs when groove angle is

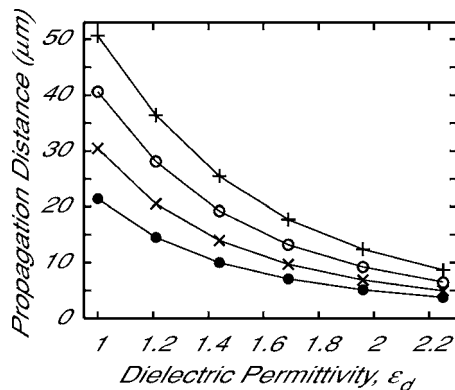


FIG. 9. The dependencies of propagation distance (at which the electric field amplitude decreases  $e$  times) for the fundamental CPP mode on dielectric permittivity  $\epsilon_d$  in a V groove with the tip radius  $r \approx 2.24$  nm in silver at  $\lambda_{\text{vac}} = 632.8$  nm for different groove angles:  $\gamma = 30^\circ$  (●),  $\gamma = 35^\circ$  (×),  $\gamma = 40^\circ$  (○), and  $\gamma = 45^\circ$  (+).

decreased (see also Ref. 14). Both these effects are explained by increased localization of the CPP mode, resulting in increasing contribution of the dissipative effects in the metal. Note, however, that for all the structural parameters considered in Fig. 9, dissipative effects in the fundamental CPP mode are still sufficiently weak to achieve propagation at least within several plasmon wavelengths. For example, the smallest propagation distance shown in Fig. 9 corresponds to  $\sim 12$  plasmon wavelengths, while the largest propagation distance corresponds to  $\sim 85$  plasmon wavelengths. Therefore, these propagation distances are assumed to be sufficient for the design of subwavelength plasmonic interconnectors between optical devices on the nanoscale. In addition, the information presented in Fig. 9 allows us to determine a reasonable trade-off between the achievable subwavelength localization and required propagation distance in a plasmonic interconnector.

## V. CONCLUSIONS

We have demonstrated that the presence of a dielectric medium inside the V groove guiding CPP modes may have a substantial impact on the plasmon propagation parameters, including the existence conditions, dispersion, localization, and typical propagation distances. In particular, it has been demonstrated that increasing dielectric permittivity in the groove results in a significant increase of both the critical groove angles which determine a range of groove angles for which CPP modes can be supported by the groove. As a result, increasing dielectric permittivity in the groove also leads to a rapid increase of localization the CPP modes. Typical penetration depths (localization regions) up the groove have also been determined and analyzed, presenting new important information about the typical depths of the groove that are required for efficient guiding of the fundamental CPP mode. The effect of such structural imperfections as rounded tips of the V grooves on the propagation parameters and properties of the CPP modes have also been investigated numerically, demonstrating that the impact of the rounded tip significantly increases with increasing dielectric permittivity in the groove (which is related to increasing localization of

the CPP modes). Typical propagation distances in all considered structures are shown to exceed at least several plasmon wavelengths, which is expected to be sufficient for nanooptics applications.

The obtained results will be important for practical development and applications of the groove subwavelength waveguides in integrated nanooptics. The conducted analysis opens new fabrication possibilities for groove plasmonic waveguides. For example, a V groove filled with dielectric can be fabricated by means of making a sharp dielectric wedge which is then covered in metal film. The conducted analysis provides important information about the expected performance of such subwavelength plasmonic waveguides.

## ACKNOWLEDGMENTS

The author would like to acknowledge the support from the Queensland Government through the Innovation Funds Smart State Ph.D. Scholarship Program and High-Performance Computing Division at the Queensland University of Technology. The authors would also like to thank Dr. Galina Gramotnev for her assistance with the statistical analysis of numerical results.

- <sup>1</sup>W. L. Barnes, A. Dereux, and T. W. Ebbesen, *Nature (London)* **424**, 824 (2003).
- <sup>2</sup>K. Tanaka and M. Tanaka, *Appl. Phys. Lett.* **82**, 1158 (2003).
- <sup>3</sup>K. Tanaka, M. Tanaka, and T. Sugiyama, *Opt. Express* **13**, 256 (2005).
- <sup>4</sup>B. Wang and G. P. Wang, *Appl. Phys. Lett.* **85**, 3599 (2004).
- <sup>5</sup>D. F. P. Pile, T. Ogawa, D. K. Gramotnev, Y. Matsuzaki, K. C. Vernon, K. Yamaguchi, T. Okamoto, M. Haraguchi, and M. Fukui, *Appl. Phys. Lett.* **87**, 261114 (2005).
- <sup>6</sup>G. Veronis and S. Fan, *Opt. Lett.* **30**, 3359 (2005).
- <sup>7</sup>L. Liu, Z. Han, and S. He, *Opt. Express* **13**, 6645 (2005).
- <sup>8</sup>G. Veronis and S. Fan, *Appl. Phys. Lett.* **87**, 131102 (2005).
- <sup>9</sup>R. Buckley and P. Berini, *Opt. Express* **15**, 12174 (2007).
- <sup>10</sup>D. F. P. Pile, T. Ogawa, D. K. Gramotnev, T. Okamoto, M. Haraguchi, M. Fukui, and S. Matsuo, *Appl. Phys. Lett.* **87**, 061106 (2005).
- <sup>11</sup>D. F. P. Pile, D. K. Gramotnev, M. Haraguchi, T. Okamoto, and M. Fukui, *J. Appl. Phys.* **100**, 013101 (2006).
- <sup>12</sup>M. Yan and M. Qiu, *J. Opt. Soc. Am. B* **24**, 2333 (2007).
- <sup>13</sup>I. V. Novikov and A. A. Maradudin, *Phys. Rev. B* **66**, 035403 (2002).
- <sup>14</sup>D. F. P. Pile and D. K. Gramotnev, *Opt. Lett.* **29**, 1069 (2004).
- <sup>15</sup>D. K. Gramotnev and D. F. P. Pile, *Appl. Phys. Lett.* **85**, 6323 (2004).
- <sup>16</sup>D. F. P. Pile and D. K. Gramotnev, *Appl. Phys. Lett.* **86**, 161101 (2005).
- <sup>17</sup>D. F. P. Pile and D. K. Gramotnev, *Opt. Lett.* **30**, 1186 (2005).
- <sup>18</sup>S. I. Bozhevolnyi, V. S. Volkov, E. Devaux, and T. W. Ebbesen, *Phys. Rev. Lett.* **95**, 046802 (2005).
- <sup>19</sup>V. S. Volkov, S. I. Bozhevolnyi, E. Devaux, and T. W. Ebbesen, *Appl. Phys. Lett.* **89**, 143108 (2006).
- <sup>20</sup>S. I. Bozhevolnyi, V. S. Volkov, E. Devaux, J.-Y. Laluet, and T. W. Ebbesen, *Nature (London)* **440**, 508 (2006).
- <sup>21</sup>E. Moreno, F. J. Garcia-Vidal, S. G. Rodrigo, L. Martin-Moreno, and S. I. Bozhevolnyi, *Opt. Lett.* **31**, 3447 (2006).
- <sup>22</sup>V. S. Volkov, S. I. Bozhevolnyi, E. Devaux, J.-Y. Laluet, and T. W. Ebbesen, *Nano Lett.* **7**, 880 (2007).
- <sup>23</sup>S. I. Bozhevolnyi, V. S. Volkov, E. Devaux, J.-Y. Laluet, and T. W. Ebbesen, *Appl. Phys. A: Mater. Sci. Process.* **89**, 225 (2007).
- <sup>24</sup>M. L. Brongersma, R. Zia, and J. A. Schuller, *Appl. Phys. A: Mater. Sci. Process.* **89**, 221 (2007).
- <sup>25</sup>D. F. P. Pile, *Appl. Phys. B: Lasers Opt.* **81**, 607 (2005).
- <sup>26</sup>N. A. Issa and R. Guckenberger, *Int. J. Exergy* **2**, 31 (2007).
- <sup>27</sup>S. I. Bozhevolnyi, *Opt. Express* **14**, 9467 (2006).
- <sup>28</sup>D. K. Gramotnev, *J. Appl. Phys.* **98**, 104302 (2005).
- <sup>29</sup>D. F. P. Pile and D. K. Gramotnev, *Appl. Phys. Lett.* **89**, 041111 (2006).
- <sup>30</sup>D. K. Gramotnev, D. F. P. Pile, M. W. Vogel, and X. Zhang, *Phys. Rev. B* **75**, 035431 (2007).
- <sup>31</sup>E. D. Palik, *Handbook of Optical Constants of Solids* (Academic, New York, 1985).